

Oxidation Chemistry of 1,3-Dimethylxanthine at Stationary Pyrolytic Graphite Electrode

Rajendra N. Goyal* and Naveen K. Singhal

Department of Chemistry, University of Roorkee, Roorkee-247667, India

(Received June 16, 1997)

The electrochemical oxidation of 1,3-dimethylxanthine has been studied in the pH range 2.3—10.3 at a pyrolytic graphite electrode. The conjugate base has been found as the electroactive species oxidized over the entire pH range. The $4e$, $4H^+$ charge transfer step is followed by competitive irreversible chemical reactions. The decomposition of UV-absorbing intermediate generated during the electrooxidation has been found to follow first-order kinetics. The products of the EC reaction have been separated by HPLC and gel-permeation chromatography and characterized by mp, 1H NMR, and mass spectra. The presence of methyl groups at positions 1 and 3 has been found to affect the course of mechanism, because the positive charge developed on nitrogen does not permit ring contraction. A tentative mechanism has also been suggested.

1,3-Dialkylxanthines have been claimed to be the best antagonists for binding to adenosine receptors, due to their high potencies as adenosine antagonists.¹⁾ They also inhibit many pharmacological and physiological effects of adenosine such as hypotensive, cardiodepressive, antidiuretic and antilipolytic effects.^{2,3)} The naturally occurring xanthines, caffeine and theophylline are the best known antagonists of adenosine receptors; however, they are non selective.⁴⁾ As electrochemical studies coupled with spectral studies have been found useful in probing the mechanistic pathway of oxidation of biomolecules,^{5–7)} it was considered desirable to study the electro-oxidation of a dialkylxanthine, viz., 1,3-dimethylxanthine at stationary pyrolytic graphite electrode. It is believed that these studies will provide some information about the metabolic pathway involved in inactivation of adenosine by xanthines, which is still an important but poorly resolved question. A detailed interpretation of the redox mechanism of 1,3-dimethylxanthine (**1**) is presented in this paper (Chart 1).

Experimental

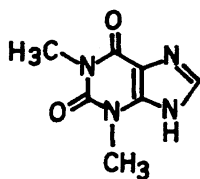
1,3-Dimethylxanthine was obtained from Research Biochem. Inc., Ma, USA. and 1,3-dimethyluric acid was a product of Aldrich Chemical Co., USA. Voltammetric studies were carried out in phosphate buffers⁸⁾ of ionic strength 0.5 M ($1\text{ M} = 1\text{ mol dm}^{-3}$). All potentials are referred to the SCE at an ambient temperature

of $20 \pm 2^\circ\text{C}$. The pyrolytic graphite electrode (PGE) used as the working electrode was prepared in the laboratory by the method reported earlier⁹⁾ and had an area of ca. 8 mm^2 . The voltammetric instruments used were essentially the same as those described earlier.¹⁰⁾ The spectral studies were carried out using a Beckman DU-6 spectrophotometer.

The stock solution (1.0 mM) of 1,3-dimethylxanthine was prepared in double distilled water; 2 ml of the stock solution was mixed with 2 ml of the buffer of desired pH. Nitrogen gas was bubbled for 10–12 min before recording voltammograms.

Controlled potential electrolysis was carried out in a conventional H-cell at a potential 100 mV more positive than peak I_a . The working electrode was a pyrolytic graphite plate ($6\text{ cm} \times 1\text{ cm}$) and the auxiliary and reference electrodes were platinum gauze and SCE respectively. The progress of electrolysis was monitored by recording cyclic voltammograms at different time intervals. The products of electrooxidation were characterized at pH 3.0 and 7.0. For this purpose, about 10 mg of the compound was electrolyzed. The progress of electrooxidation was monitored by observing the decrease in peak I_a in cyclic voltammetry. When peak I_a completely disappeared, the exhaustively electrolyzed solution was removed from the cell and lyophilized. The freeze dried material was dissolved in 1–2 ml of water and passed through a glass column packed with Sephadex G-10 (Sigma; bead size $40\text{--}120\text{ }\mu\text{m}$). Double distilled water was used as an eluent and the fractions of 5 ml each were collected. The absorbance of the fractions was monitored at 210 nm. The absorbance versus volume plot exhibited two peaks at pH 7.0. The first peak P_1 (140–180 ml) was found to contain phosphate and hence discarded. The volume under peak P_2 (220–240 ml) was collected, lyophilized and a colorless material was obtained.

The progress of electrooxidation of 1,3-dimethylxanthine was monitored at pH 3.0 by High-performance liquid chromatography (HPLC) employing a Shimadzu model SPD-10A. For HPLC studies, 1 mM solution of compound **1** was oxidized at pH 3.0 (adjusted by adding dilute HCl). $5.0\text{ }\mu\text{l}$ of the solution was injected in a reversed phase C_{18} column to which a pre-column was attached. The mobile phase solvent was methanol (AR) and the flow rate was 0.50 ml min^{-1} . The absorbance of the eluent was monitored at 215 nm.



(1)

Chart 1.

The column was equilibrated for 20 min before the next injection was made.

The mass spectra were recorded using a JEOL, JMS D 300 instrument and the ^1H NMR were recorded using a Varian XL 300 spectrometer in CDCl_3 . Silylation was carried out in a 3.0 ml Vial (Pierce Chemical Co., USA) by treating 50–100 μg of the product with 50 μl of *N,N*-bis(trimethylsilyl)trifluoroacetamide (BSTFA) and 50 μl of acetonitrile at 110 $^\circ\text{C}$ for 10 min. The vial was cooled and 2 μl of the sample was injected in GC/Mass

Results and Discussion

Linear sweep voltammetry of 0.5 mM 1,3-dimethylxanthine exhibited a well-defined anodic peak (Ia) in the pH range 2.3–10.3 at a sweep rate of 20 mV s^{-1} . The peak potential of peak Ia was dependent on pH and shifted to less positive potential with increase in pH. The plot of E_p versus pH exhibited a break at around pH 8.6 (Fig. 1) which corresponds to the $\text{p}K_a$ value of 1,3-dimethylxanthine as reported in the literature.¹¹⁾ The dependence of E_p on pH can be expressed by the relations:

$$E_p (\text{pH } 2.3\text{--}8.6) = [1420 - 62.5 \text{ pH}] \text{ mV vs. SCE}$$

$$E_p (\text{pH } 8.6\text{--}10.3) = [1050 - 28.0 \text{ pH}] \text{ mV vs. SCE}$$

The dependence of E_p on pH in the pH range 8.6–10.3 clearly suggests that the electroactive species is not the species present in the bulk of the solution, but its conjugate base bearing one less proton. The slope of ca. 60 mV/pH corresponds to the same number of electrons and protons in the pH range 2.3–8.6, whereas a lower number of protons are consumed at $\text{pH} > 8.6$. The $\text{p}K_a$ 8.6 thus represents dissociation of NH proton from position 9. The presence of methyl groups at positions 1 and 3 not only restricts the tautomerism but also produces an inductive effect (Chart 2). As fully methylated pyrimidine rings in purines are mesomeric,

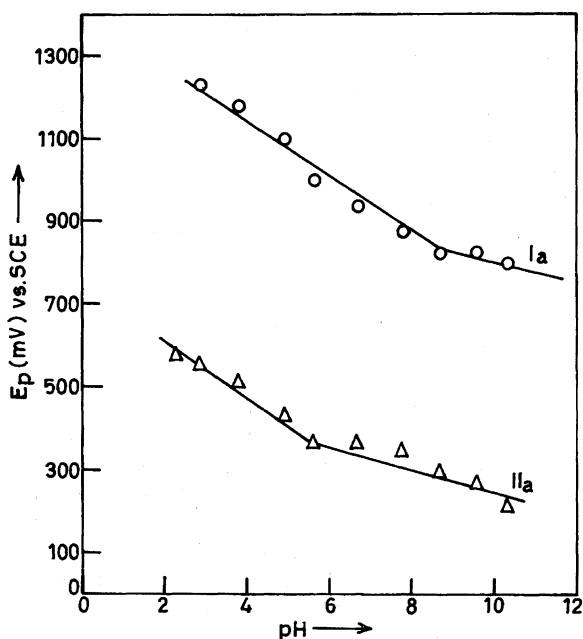


Fig. 1. Dependence of peak potential on pH for the oxidation peaks of 1,3-dimethylxanthine sweep rate 20 mV s^{-1} .

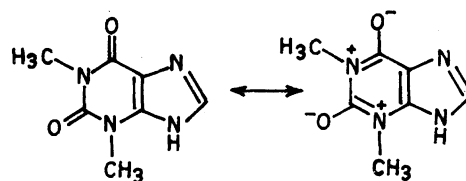


Chart 2.

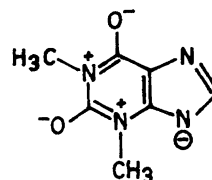


Chart 3.

the following canonical forms must contribute in the bulk of the solution. Similar canonical forms have been suggested on the basis of bond length measurements by Sutor.^{12,13)}

Hence, the species predominating at $\text{pH} > 8.6$ should be an anion formed by the loss of a proton from position 9 (Chart 3).

Cyclic sweep voltammetry of 1,3-dimethylxanthine at a sweep rate of 100 mV s^{-1} also exhibited a well-defined oxidation peak (Ia) in the pH range 2.3–10.3, when the sweep was initiated in the positive direction. Peak Ia was clearly observed at a sweep rate $\leq 150 \text{ mV s}^{-1}$; at higher sweep rates, peak Ia turned to a bump and merged with the background.

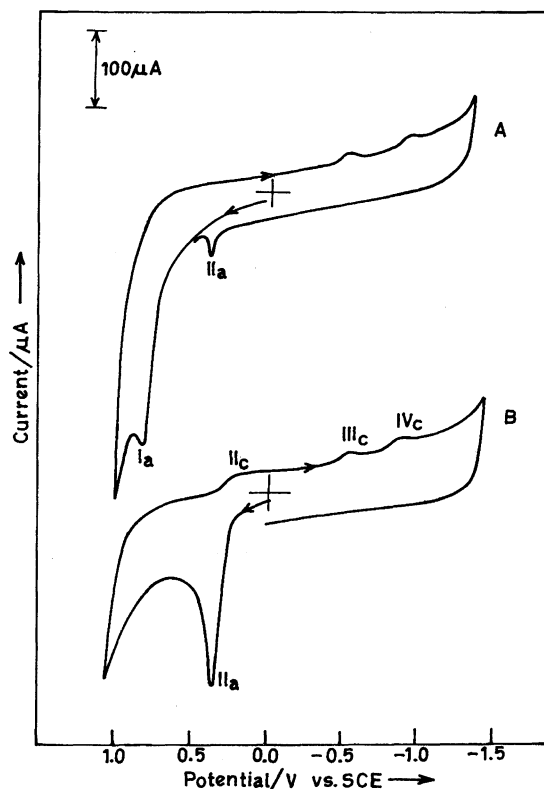


Fig. 2. Typical cyclic voltammograms of 0.5 mM 1,3-dimethylxanthine (A) and 1,3-dimethyluric acid (B) at pH 7.0, sweep rate 100 mV s^{-1} .

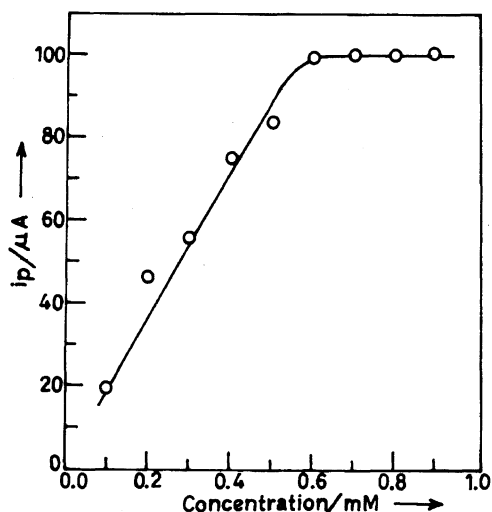


Fig. 3. Observed dependence of peak current on concentration for the peak IIa of 1,3-dimethylxanthine at pH 7.0.

When the direction of the sweep was reversed, two reduction peaks (IIIc and IVc) were noticed. On further reversing the sweep a new oxidation peak IIa appeared at a less positive potential. Some typical cyclic voltammograms of 1,3-dimethylxanthine are depicted in Fig. 2. The peak potential of peak IIa was also dependent on pH and shifted to a less positive potential with increases in pH. The E_p -pH dependence for peak IIa is presented in Fig. 1 and showed a break at ca. pH 5.6. The ratio of peak currents Ia/IIa was practically constant (2.5–2.8) over the entire pH range.

The effect of concentration on peak current was studied in the concentration range 0.1 to 1.0 mM. The peak Ia current increased with increase in concentration of 1,3-dimethylxanthine. The i_p versus concentration plot indicated a linear increase up to about 0.6 mM concentration; at higher con-

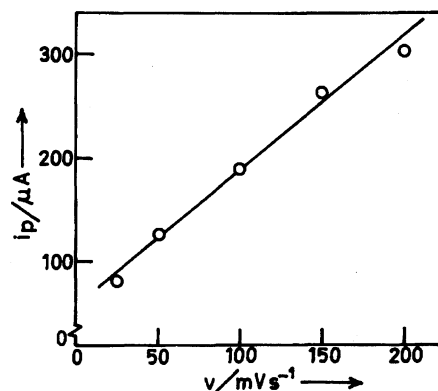


Fig. 4. Dependence of peak current on sweep rate for the peak IIa of 1,3-dimethylxanthine.

centrations, the i_p value became practically independent of concentration (Fig. 3). This behavior suggested the adsorption of 1,3-dimethylxanthine at the surface of PGE.¹⁴⁾

The adsorption of 1,3-dimethylxanthine at the electrode surface was further confirmed¹⁵⁾ by the increase in peak current (i_p) with increase in sweep rate (Fig. 4). The ratio of peaks Ia/IIa was found to be ca. 3.0 over the entire concentration range studied.

The effect of sweep rate on peak Ia was studied over the sweep range 10–200 mVs^{-1} . At a sweep rate $> 200 mVs^{-1}$, peak Ia merged with the back-ground even at pH 7.0 and hence accurate determinations of peak currents were not possible. The ratio of peaks Ia/IIa was more or less constant (ca. 3.0) in this sweep range. To evaluate the sweep rate effect in a large sweep range, studies were carried out at pH 9.0. It was noticed that the E_p of peak (Ia) shifted by 5–10 mV per ten-fold increase in sweep rate in the range 20 to 200 mVs^{-1} and decreased to 5 mV in the range 200–500

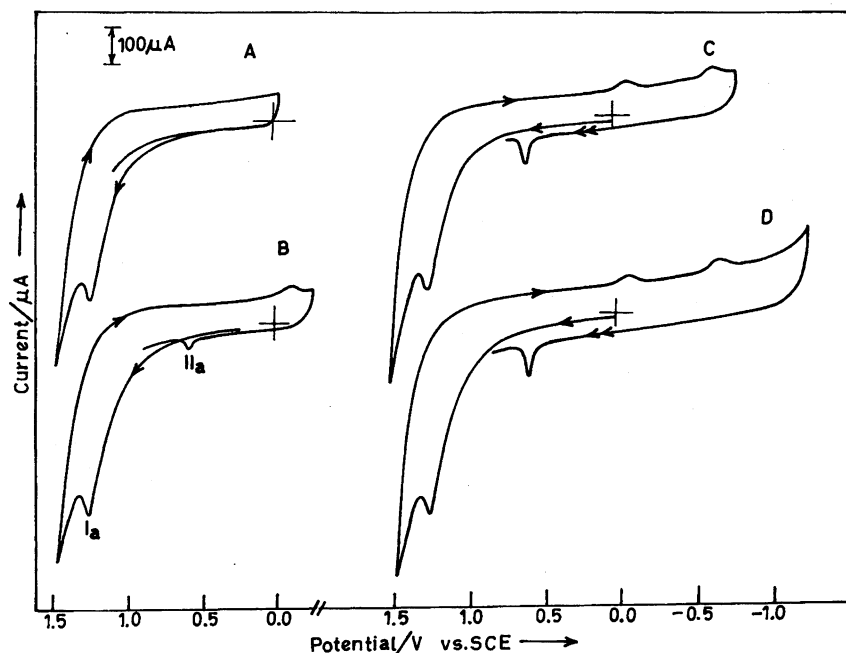


Fig. 5. Effect of potential reversal on the oxidation peak IIa of 1,3-dimethylxanthine at pH 3.0, sweep rate 100 mVs^{-1} .

Table 1. Coulometric n -Values Observed for the Electrooxidation of 1,3-Dimethylxanthine and 1,3-Dimethyluric Acid at PGE

pH	Expt. n^a		Expt. n^a	
	Potential (V) vs. SCE	1,3-Dimethylxanthine	Potential (V) vs. SCE	1,3-Dimethyluric acid
2.3	1.2	4.1	0.6	1.9
3.0	1.2	3.8	0.6	1.8
4.9	1.1	3.9	0.5	1.8
7.0	1.0	4.0	0.5	1.8
7.8	1.0	4.2	0.4	1.9
8.7	0.9	4.0	0.4	1.9
9.6	0.9	3.8	0.4	1.8
10.3	0.8	3.8	0.3	1.7

a) Average of at least two replicate determinations.

mV s^{-1} . At sweep rates greater than 500 mV s^{-1} , peak Ia again merged with the background. The plot of $\Delta E_{p/2}$ versus $\log v$ was found to be S-shaped. Hence it was concluded that the nature of the electrode reaction was EC, in which charge transfer is followed by irreversible chemical reactions.^{16,17)}

The electrochemical oxidation of xanthine has been found to proceed via uric acid.¹⁸⁾ It was thus considered interesting to check whether the electrooxidation of 1,3-dimethylxanthine also proceeds through the formation of 1,3-dimethyluric acid or not. For this purpose, cyclic voltammograms of 1,3-dimethyluric acid were recorded under identical conditions in the pH range 2.3–10.3. A well-defined peak Ia is observed with the same $dE_p/d\text{pH}$ as was obtained for peak IIa

in the case of 1,3-dimethylxanthine. Hence, it is concluded that peak IIa of 1,3-dimethylxanthine is due to the formation of 1,3-dimethyluric acid in the electrode reactions.

To determine whether 1,3-dimethyluric acid, a species responsible for peak IIa, is generated by the oxidation reaction of peak Ia or the reduction reaction of peak IIIc/IVc, cyclic voltammograms were recorded by changing the direction of the negative-going sweep at different potentials. It was noticed that peak IIa did not appear if the direction of sweep is reversed before peak IIIc (Fig. 5A). However, if the sweep is extended to more negative potentials, peak IIa systematically increased. (Figs. 5B to D). Thus, it is concluded that 1,3-dimethyluric acid is generated by the reduction of peak Ia

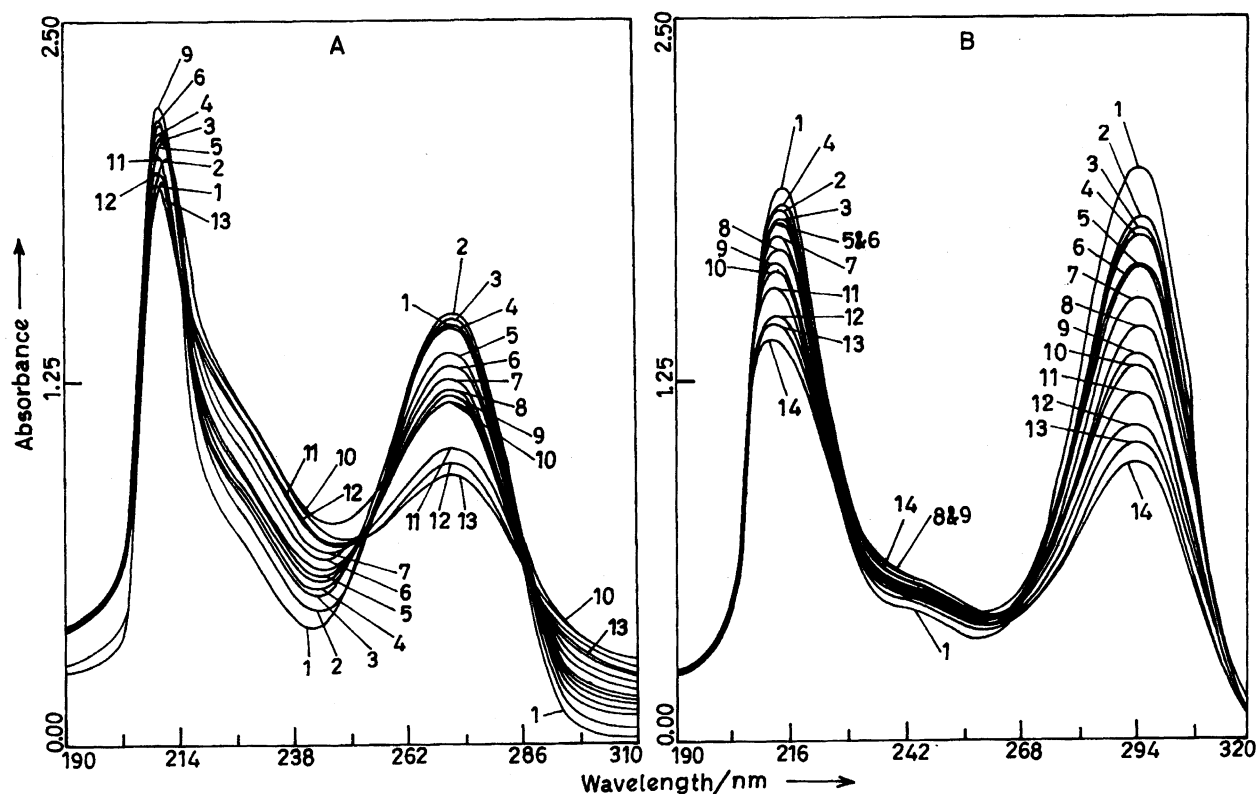


Fig. 6. Spectral changes observed at pH 7.0 during electrooxidation of (A) 0.1 mM 1,3-dimethylxanthine, Pot 1.0 V vs. SCE and (B) 0.1 mM 1,3-dimethyluric acid, Pot 0.5 V vs. SCE. Curves were recorded at an interval of 5 min.

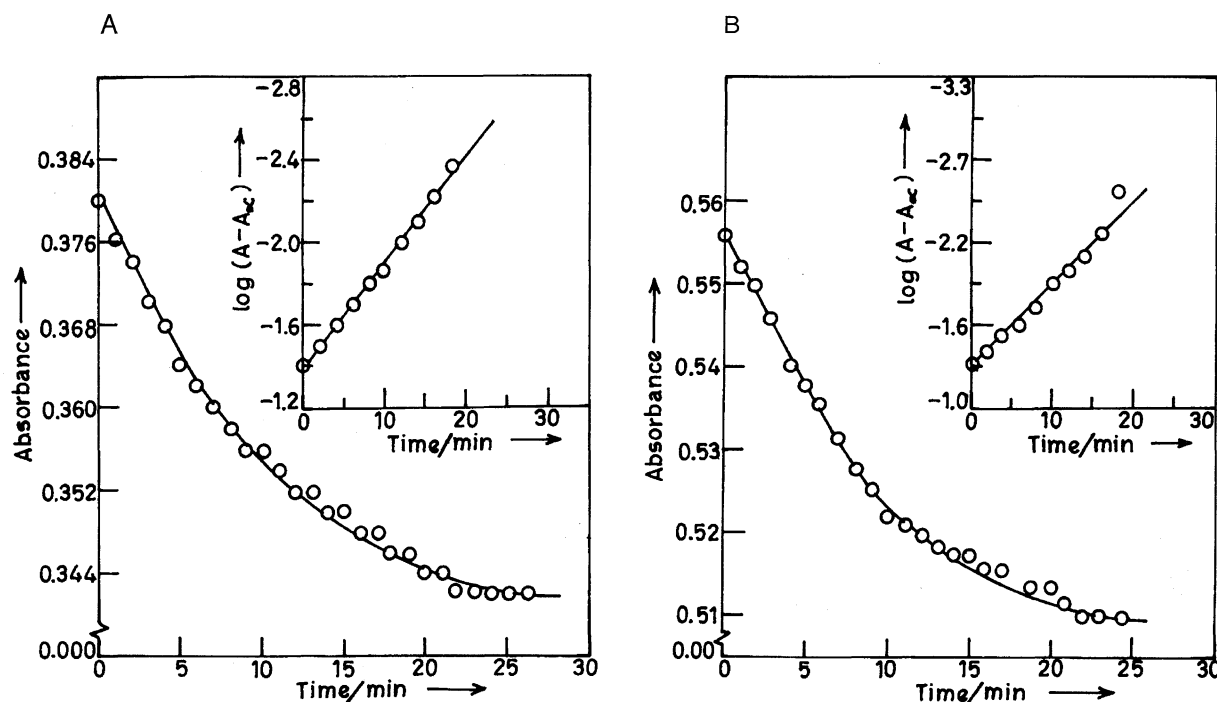


Fig. 7. Change of absorbance vs. time and $\log(A - A_\infty)$ vs. time observed at pH 7.0 at 270 nm for 1,3-dimethylxanthine (A) and 1,3-dimethyluric acid (B).

product and not during the oxidation of peak Ia process.

Controlled potential electrolysis of 0.5 mM 1,3-dimethylxanthine was carried out in a conventional H cell. The nature of i_p versus time plot was exponential, however, the plot of $\log i_p$ versus time was a straight line only for the first 10–12 min of electrolysis, after which a large deviation was noticed. The deviation from the straight line clearly indicated that the electrode reaction followed a simple path only for the first 10–12 min, after which the follow-up chemical reactions played a significant role in the bulk cleavage of the products, as has been suggested by Cauquis¹⁹⁾ and others.²⁰⁾ The values of n , numbers of electrons involved in oxidation, were determined by connecting a coulometer in series; the value of n was found as 4.0 ± 0.2 in the entire pH-range studied. The values of n observed at different pH are presented in Table 1. The n -values observed for 1,3-dimethyluric acid on the other hand were 1.8 ± 0.2 in the entire pH range studied. However, the $\log i_p$ versus time plot was a straight line only for the first 8–10 min of oxidation. Thus, the follow-up chemical reactions were also found to play a significant role during the electro-oxidation of 1,3-dimethyluric acid.

Spectral Studies. UV spectra of 0.1 mM 1,3-dimethylxanthine were recorded in the pH range 2.3–10.3 to determine the pK_a . In the entire pH range studied, 1,3-dimethylxanthine exhibited two well defined λ_{\max} at around 210 and 270 nm and a shoulder at 223 nm. The absorbance at 270 nm was plotted against pH. The resulting dissociation curve gave an inflection at around pH 8.6, corresponding to the pK_a of 1,3-dimethylxanthine as reported in the literature.¹¹⁾ The pK_a determined spectrophotometrically was also similar to the value obtained from the E_p –pH relation.

Spectral changes during electrochemical oxidation of 1,

3-dimethylxanthine were monitored at pH 3.0 and 7.0. A typical UV-spectrum of 1,3-dimethylxanthine at pH 7.0 is presented by curve 1 in Fig. 6 and shows two maxima at 210 and 270 nm. When a potential 100 mV more positive than peak Ia is applied, the absorbance at 270 nm first increased and then a systematic decrease in absorbance was noticed. The absorbance in the region 214–250 nm systematically increased for the first 45 min of electrolysis and then the absorbance decreased. The absorbance at shorter wavelength maximum (210 nm) first increased, shifted to 208 nm and increased for 45 min, and then decreased. Similarly, the absorbance in the longer wavelength region increased for the first 45 min and then decreased. The absence of a clear isosbestic point at 252 and 285 nm is most likely due to the involvement of competitive chemical reactions. If the potential is turned off at any stage during electrolysis, the absorbance in the region 225–310 nm showed a decreasing trend.

The kinetic study of the decomposition of the UV-absorbing intermediate was carried out at selected wavelengths. For this purpose, the electrolysis was terminated when the absorbance at λ_{\max} reached to about 50%. The absorbance of the intermediate species was monitored as a function of time and the resulting curves were exponential in nature (Fig. 7). The plots of $\log(A - A_\infty)$ versus time were linear at all the pH values and hence suggested that the decomposition reaction of the UV-absorbing intermediate followed first-order kinetics. The values of k calculated from $\log(A - A_\infty)$ versus time plots at different pH were in the range 1.9 – $2.5 \times 10^{-3} \text{ s}^{-1}$ and are summarized in Table 2.

As cyclic voltammetric studies indicated that peak IIa is due to the formation of 1,3-dimethyluric acid, spectral

Table 2. Comparison of Rate Constant Values (k) Observed for the Decay of UV-Absorbing Intermediate for 1,3-Dimethylxanthine and 1,3-Dimethyluric Acid

pH	λ/nm	1,3-Dimethylxanthine		1,3-Dimethyluric acid	
		Pot. (V)	$k \times 10^{-3} \text{ s}^{-1}$ ^{a)}	Pot. (V)	$k \times 10^{-3} \text{ s}^{-1}$ ^{a)}
4.0	235	1.20	2.0	0.70	1.9
	270		1.9		2.1
	295		1.9		1.9
7.0	235	1.00	2.1	0.60	2.2
	270		1.9		2.1
	295		1.9		2.1
8.0	235	1.00	1.9	0.60	1.9
	270		2.4		1.9
	295		2.5		2.1

a) Average of at least three replicate determinations.

changes were also monitored during electro-oxidation of 1, 3-dimethyluric acid at pH 7.0 and two well-defined bands at λ_{max} 214 and 292 nm were observed. Upon application of a more positive potential to peak IIa, a systematic decrease in absorbance at both the λ_{max} was noticed. However, absorbance in the region 226–268 first increased (curves 8, 9) then decreased and became constant. If potential is turned off after recording curve 8, the absorbance at both the λ_{max} decreased (Fig. 6B). The values of k for the first order decay of the UV-absorbing intermediate were calculated from $\log(A - A_{\infty})$ versus time plots and are summarized in Table 2. It was interesting to note that the values of k for 1, 3-dimethylxanthine and 1,3-dimethyluric acid were essentially similar and hence the same UV-absorbing intermediate species is generated in both cases. The UV-spectral changes for 1,3-dimethylxanthine at pH 3.0 were basically similar to pH 7.0.

Product Isolation and Characterization. The products

of electro-oxidation of 1,3-dimethylxanthine were separated by High performance liquid chromatography at pH 3.0. The chromatograms observed during the electrooxidation of 1,3-dimethylxanthine are presented in Fig. 8. Curve A presents the chromatogram of 1,3-dimethylxanthine just before the oxidation; a well-defined peak at $R_t \approx 7.1$ min was noticed. With progress of electrolysis, two new peaks (1 and 3) were observed at $R_t \approx 5.0$, and 7.5 min (Fig. 8, Curve B). The HPLC peaks at $R_t \approx 7.1$ min completely disappeared after 3 h of electrolysis. To collect the material obtained under peaks 1 and 3, several injections were made in HPLC and the volume was collected separately under the peaks and lyophilized. The colorless dried material obtained under each peak was characterized by mp, ^1H NMR, and mass spectra.

HPLC Peak 1: The colorless material obtained from peak 1 had a mp of 134 °C. The FT-IR spectrum of this material exhibited sharp bands at 3385, 3490, and 1675 cm^{-1} and was practically identical to the FT-IR of authentic urea. The

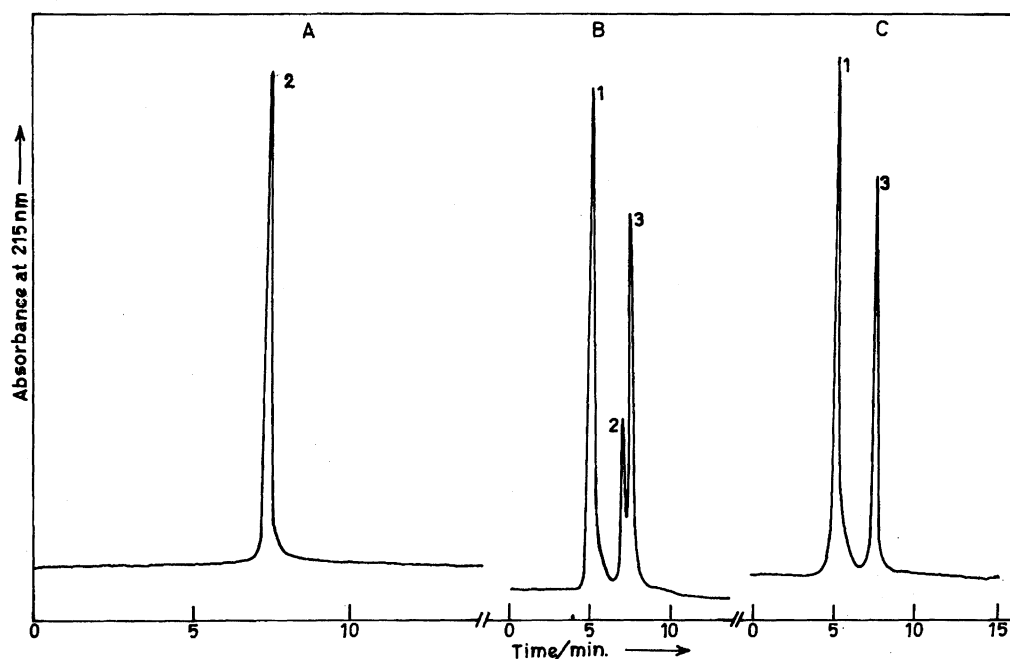
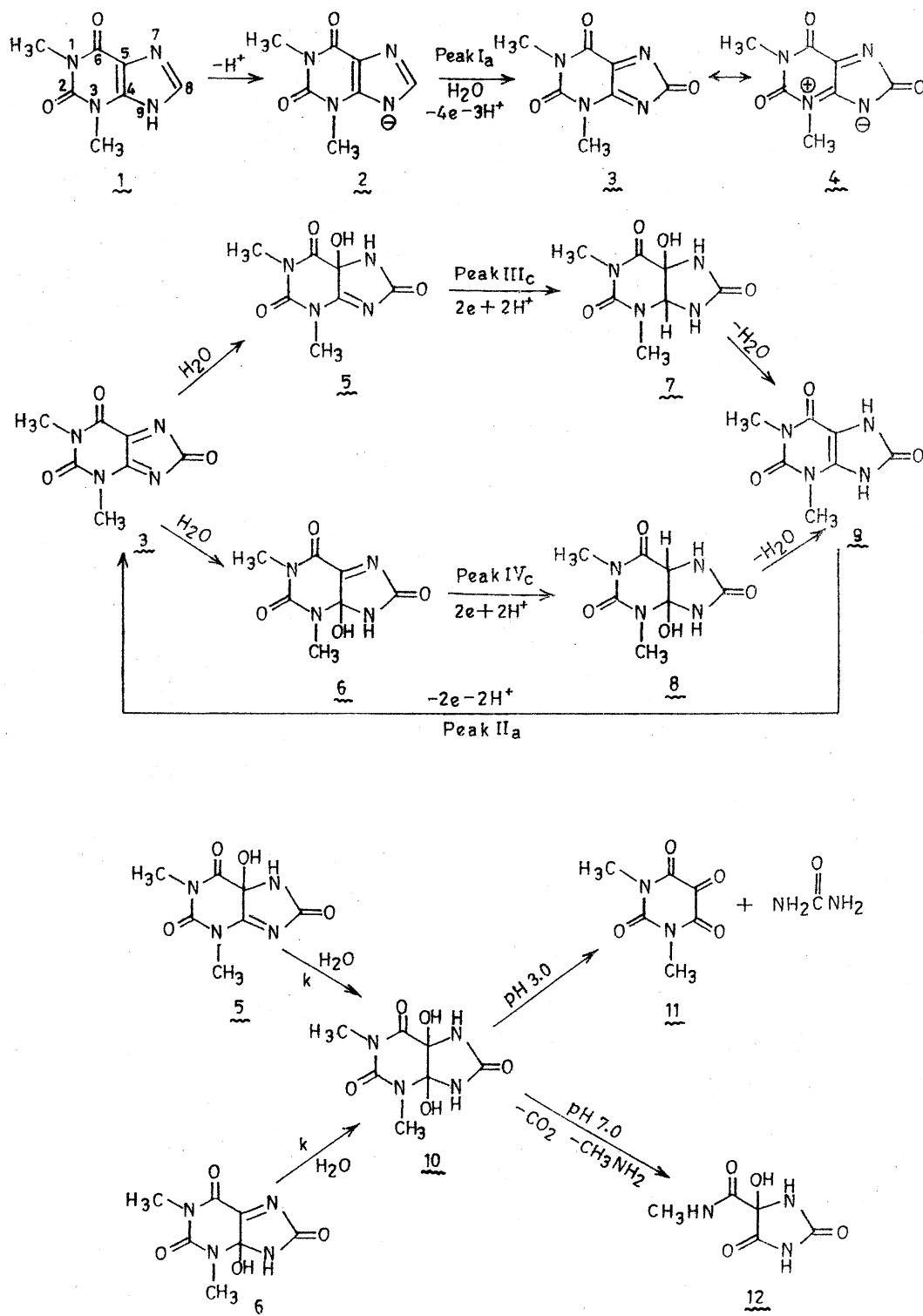


Fig. 8. HPLC chromatograms observed during electrooxidation of 1,3-dimethylxanthine at pH 3.0 curves were recorded at 0 min (A), 1 h (B), and 3 h (C) of electrolysis.



Scheme 1.

mass spectrum of this material exhibited a clear molecular ion peak at $m/z=60$ (100%) and hence it was concluded that the product is urea.

The formation of urea as one of the products suggested that the imidazole ring of 1,3-dimethylxanthine ruptures at pH 3.0 to give the products. The imidazole ring opening of purines has also been reported during chemical oxidation using a variety of reagents.^{21,22} Hence, the other product

formed should be an alloxan derivative.

HPLC Peak 3: The volume collected under HPLC peak 3 on lyophilization gave a colorless material having mp 220 °C. The mass spectrum of this material gave a clear molecular ion peak at $m/z=170$ (96.8%), indicating the molar mass of the material was 170. The major peaks in the mass spectrum were noticed at 172 (1.1%), 171 (7.3%), 170 (96.8%), 143.9 (0.6%), 142.9 (50%), 142 (76.2%), 115

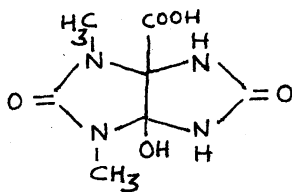


Chart 4.

(3.4%), 114 (61.9%), 87 (1%), 86.1 (22.6%), and 70 (56.9%). The ^1H NMR spectrum of the material exhibited signals at $\delta=7.9$ (s, 2H); 3.4 (s, 3H), and 3.2 (s, 3H). On adding D_2O , the signal at $\delta=7.8$ disappeared and hence was assigned to water protons. The material was thus characterized as 1,3-dimethylalloxan monohydrate.

The exhaustively electrolyzed solution of 1,3-dimethylxanthine at pH 7.0 exhibited only single spot in TLC ($R_f\approx 0.45$); hence the product of electrooxidation was separated from the buffer constituents by using gel-permeation chromatography (see Experimental). The colorless material obtained under the chromatographic peak P_2 (220–240 ml) had a mp 184 °C. The mass spectrum of the material exhibited a relatively small molecular ion peak at m/z 173 (20%). To further confirm the molar mass as 173, the material was silylated using BSTFA and acetonitrile. The derived sample gave a peak at $R_t\approx 24$ min in GC which exhibited a clear molecular ion peak m/z 389 (76.4%). The molar mass of 389 corresponded to the trisilylated molecule. Hence, this product was characterized as 4-hydroxy-2,5-dioxoimidazolidine-4-(*N*-methylcarboxamide).

The formation of 4-hydroxy-2,5-dioxoimidazolidine-4-(*N*-methylcarboxamide) as a product of oxidation of 1,3-dimethylxanthine at pH 7.0 is not unusual, as 5-hydroxy hydantoin-5-carboxamide has been obtained from the electrooxidation of uric acid.²³⁾ It is expected that 4-hydroxy-2,5-dioxo-4-imidazolidinecarboxamide should give tetrasilylated species on treatment with BSTFA and acetonitrile. However, due to steric hindrance, the $-\text{OH}$ group present between $\text{C}=\text{O}$ and $-\text{NH}$ does not undergo silylation, as has been observed in the case of 4-hydroxy-2,5-dioxo-4-imidazolidinecarboxamide.^{23,24)}

Thus, at pH 7.0 the pyrimidine ring of 1,3-dimethylxanthine opens to give the ultimate products. The rupture of pyrimidine ring of purines in neutral and alkaline media during chemical oxidation has been well documented in the literature.²⁵⁾

The E_p -pH dependence clearly indicates that the conjugate base is the electroactive species of 1,3-dimethylxanthine. It is expected that $dE_p/d\text{pH}$ of ca. 60 mV/pH and 30 mV/pH corresponds to the number of protons of four and two respectively. Scheme 1 depicts 4H^+ in the conversion of 1 to 3 and 3H^+ in the conversion of 2 to 3. Thus, the slope of $dE_p/d\text{pH}$ expected at $\text{pH}>8.6$ is 45 mV/pH. The lesser value of the slope observed may be due to a limited number of points in Fig. 1. Thus, the initial peak Ia involves a $4e$, 3H^+ step to give the corresponding diimine 3, similar to the basic reaction proposed earlier for xanthine.¹⁸⁾ The unstable diimine 3 can exist in two canonical forms 4 and could not

be detected by the cyclic voltammetry even at fast sweep rate ($>5\text{ V s}^{-1}$). Thus, the peak Ia seems to be an irreversible process leading to the formation of diimine. The peak Ia appears on the anodic background currents (Fig. 2) and is due to oxidation of species adsorbed on the electrode surface. If adsorbed species is involved in the electrochemical oxidation, bulk electrolysis is impossible. Thus, the background currents show electrooxidation of 1,3-dimethylxanthine dissolved in the electrolyte, and the adsorbed one exhibits the voltammogram peak. The diimines obtained in purine oxidations have been found to be very unstable due to two $\text{C}=\text{N}$ bonds. The half life of diimine obtained in uric acid oxidation has been found to be 20 ms.²⁶⁾ Thus, it is expected that the diimine 3 would also be unstable and would be readily attacked by the water molecule in a chemical follow up step to give imine alcohol. As there are two $\text{C}=\text{N}$ bonds in diimine 3, the hydration can occur at either of the two $\text{C}=\text{N}$ bonds to give imino alcohol 5 or 6. The reduction of the latter species in $2e$, 2H^+ step, (peak IIIc or IVc) would give dihydro molecule 7 or 8, which on losing a molecule of water will give 1,3-dimethyluric acid. At this stage, it is difficult to establish whether conversion of imino alcohol species 5 to 7 is represented by peak IIIc or IVc. The case with the conversion of 6 to 8 is also similar. It was observed that Peak IIa is noticed only when first negative sweep is extended to Peak IIIc. Hence, conversion of 5 to 7 or 6 to 8 may be responsible for Peak IIIc. Looking at the structure of species 5 and 6, it seems more probable that reduction of species 6 would occur at high negative potentials in comparison to species 5, due to steric hindrance of $-\text{CH}_3$ group.

The further hydration of imino alcohol species 5 and 6 appears to be responsible for the decay observed in the first order reaction to give diol 10. At pH 3.0, the imidazole ring opens to give, 1,3-dimethylalloxan 11 and urea, whereas at pH 7.0 the pyrimidine ring breaks and decarboxylation gives 4-hydroxy-2,5-dioxoimidazolidine-4-(*N*-methylcarboxamide).

The observed electrochemical behavior of 1,3-dimethylxanthine appears to be little different than that of xanthine. The presence of methyl groups in pyrimidine ring not only restricts the number of resonating structures, but also produce a positive charge on pyrimidine nitrogen due to canonical structures. The positive charges on nitrogen atoms do not permit the contraction of the pyrimidine ring and hence the formation of 1-carbohydroxy-2,4-dimethyl-2,4,6,8-tetraza-3,7-dioxo-5-ene-tricyclo [3,3,0] octane, a primary requirement for the formation of allantoin (5-uriedohydantoin),²³⁾ is not fulfilled (Chart 4).

Thus, 5-(1,3-dimethyluriedo) hydantoin is not obtained as a product during electrooxidation of 1,3-dimethylxanthine. On the other hand, presence of methyl group in the imidazole ring has been reported not to affect the ring contraction and hence allantoin has been found as the product.²⁷⁾ Thus, these studies clearly indicate that presence of CH_3 group in pyrimidine ring of purines does not permit ring contraction of the diol intermediate and hence the ultimate products are different than xanthine.

Financial assistance for this work was provided by the Department of Science and Technology, New Delhi through grant number SP/SI/G21/91.

References

- 1) R. F. Bruns, J. W. Daly, and S. H. Snyder, *Proc. Natl. Acad. Sci. U.S.A.*, **77**, 5547 (1980).
- 2) B. B. Fredholm, K. Jacobson, B. Jonzon, K. Kirk, Y. Li, and J. Daly, *J. Cardiovasc. Pharmacol.*, **9**, 396 (1987).
- 3) K. A. Jacobson, L. Kiriasis, S. Barone, B. J. Bradbury, U. Kammula, J. M. Campague, S. Secunda, J. W. Daly, J. L. Neumeyer, and W. Pfeleiderer, *J. Med. Chem.*, **32**, 1873 (1989).
- 4) J. W. Daly, *J. Med. Chem.*, **25**, 197 (1982).
- 5) K. J. Volk, R. A. Yost, and A. B. Toth, *Anal. Chem.*, **64**, 21A (1992).
- 6) K. Rajeshwar, R. O. Lezna, and N. R. Tacconi, *Anal. Chem.*, **64**, 429A (1992).
- 7) R. N. Goyal, A. K. Jain, and N. Jain, *J. Chem. Soc., Perkin Trans. 2*, **1996**, 1153.
- 8) G. D. Christian and W. C. Purdy, *J. Electroanal. Chem.*, **3**, 363 (1962).
- 9) R. N. Goyal, S. K. Srivastava, and R. Agarwal, *Bull. Soc. Chim. Fr.*, **1985**, 656.
- 10) R. N. Goyal and D. K. Garg, *Bioelectrochem. Bioenerg.*, **39**, 249 (1996).
- 11) D. Lichtenberg, F. Bergmann, and Z. Neiman, *J. Chem. Soc.*, **1971**, 1676.
- 12) D. J. Sutor, *Acta Crystallogr.*, **11**, 453 (1958).
- 13) D. J. Sutor, *Acta Crystallogr.*, **16**, 97 (1963).
- 14) R. S. Nicholson and I. Shain, *Anal. Chem.*, **36**, 706 (1964).
- 15) R. H. Wopschall and I. Shain, *Anal. Chem.*, **39**, 1514 (1967).
- 16) P. H. Reiger, "Electrochemistry," Prentice Hall, Englewood Cliffs, NJ (1987), p. 343.
- 17) E. C. Brown and R. F. Large, in "Techniques of Chemistry," ed by A. Weissberger and R. W. Rossiter, Wiley, N. Y. (1974), p. 423.
- 18) R. N. Goyal, *Indian J. Chem., Sect. A*, **28A**, 467 (1989).
- 19) G. Cauquis and V. D. Parker, in "Organic Electrochemistry," ed by M. M. Baizer, Marcel Dekker, N.Y. (1973), p. 134.
- 20) L. Meites, in "Physical Methods of Chemistry," ed by A. Weissberger and R. W. Rossiter, Wiley, N. Y. (1974), p. 134.
- 21) E. Shaw, *J. Org. Chem.*, **27**, 883 (1962).
- 22) R. K. Robins, "Heterocyclic Compounds," ed by R. C. Elderfield, Wiley, N. Y. (1967), Vol. 8, p. 162.
- 23) R. N. Goyal, A. B. Toth, and G. Dryhurst, *J. Electroanal. Chem.*, **131**, 181 (1982).
- 24) A. B. Toth, R. N. Goyal, M. Z. Wrona, T. Lacava, N. T. Nguyen, and G. Dryhurst, *J. Electroanal. Chem.*, **128**, 413 (1981).
- 25) V. H. Brederick, F. Effenburger, and G. Rainer, *Ann. N. Y. Acad. Sci.*, **673**, 82 (1964).
- 26) H. A. Marsh and G. Dryhurst, *J. Electroanal. Chem.*, **95**, 81 (1979).
- 27) R. N. Goyal, V. Bansal, and M. S. Verma, *Bull. Soc. Chim. Fr.*, **130**, 146 (1993).